Studia Quaternaria, vol. 35, no. 1 (2018): 55–71

DOI: 10.2478/squa-2018-0004

RESULTS OF INTEGRATED GEOARCHAEOLOGICAL PROSPECTION OF UNIQUE IRON AGE HILLFORT LOCATED ON RADOMNO LAKE ISLAND IN NORTH-EASTERN POLAND

Fabian Welc[1*], Jerzy Nitychoruk[2], Rafał Solecki[1], Kamil Rabiega[1], Jacek Wysocki[1]

[1] *Institute of Archaeology, Cardinal Stefan Wyszyński University in Warsaw, Poland, e-mail: f.welc@uksw.edu.pl*

[2] *Pope John Paul II State School of Higher Education in Biała Podlaska, Poland, e-mail: jerzy.nitychoruk@pswbp.pl*

** corresponding author*

Abstract

Archaeology of north-eastern Poland has been poorly recognized owing to vast forest areas and numerous lakes. This particularly refers to the Warmian–Masurian Voivodship, where forest covers over 30% of its area. Prospection of forested areas has become possible in Poland just over 10 years ago with the Airborne Laser Scanning (ALS) and Light Detection and Ranging (LiDAR). These techniques allow obtaining 3-D documentation of recognized and also unknown archaeological sites in the forested areas. Thanks to ALS/LiDAR prospection a significant number of archaeological structures have been identified also in the Warmia and Masuria regions. Among them oval-shaped hillforts, surrounded by perfectly spaced concentric moats and ramparts, located mainly on islands and in wetland areas, have raised particular attention. Based on field prospection and results of preliminary excavations, these objects have been considered as Iron Age hillforts. One of the best preserved objects of this type is on the Radomno Lake island, located several kilometres to the south of Iława town. Integrated geoarchaeological prospection of this hillfort emphasized benefits of using LiDAR in combination with results of geophysical prospection and shallow drillings. Applied methodology enabled to document the hillfort shape, and to study its geological structure and stratigraphy. The results clearly indicate that integration of LiDAR data with geophysical prospecting is indispensable in future archaeological surveys. It is a perfect tool for remote sensing of archaeological objects in forest areas, so far not available for traditional archaeology.

Key words: LiDAR/ALS, GIS, geophysical methods, archaeology, Iron Age hillforts, forested areas, north-eastern Poland, Warmia and Masuria regions.

Manuscript received 29 January 2018, accepted 27 March 2018

INTRODUCTION

Till recently, archaeological resources of north-eastern Poland have only partially been recognized due to the presence of a large number of lakes and densely forested areas. This particularly applies to the Warmian–Masurian Voivodship, where forest covers about 7459 km^2, that is almost 31% of the total region surface (Report, 2013) (Fig. 1). Reliable prospection of forested areas in Poland has become possible just over 10 years ago with the Airborne Laser Scanning (ALS) and Light Detection and Ranging (LiDAR) techniques (Banaszek, 2014). Application of ALS measurements enables recognizing archaeological sites in a forest, characterized by a specific form that is manifested on the surface (Crow *et al.,* 2008). Moreover, anthropopression and natural erosion in a forest were very weak due to dense undergrowth. Accordingly, in such circumstances archaeological sites very often conserved their primary form, which is not a common case in farmlands or areas with intensive urban transformations (Doneus *et al.,* 2008).

In 2017 we have started a research project in Warmia and Masuria regions, funded by the Polish National Science Centre (NCN). Its main aim is to investigate how past humans were influenced by environmental changes. Archaeological sites located near lakes, especially those on densely forested islands, are studied within the frames of this project. Due to presence of a woody cover, the first stage of remote sensing of these sites is conducted with application of LiDAR acquired from the IT ISOK system (IT Polish System of the Country's Protection Against Extreme Hazards), available from the open public domain http://www.geoportal.gov.pl/en. This platform allows obtaining 3-D documentation of already recognized and also unknown archaeological sites (Fig. 1). Particular attention is

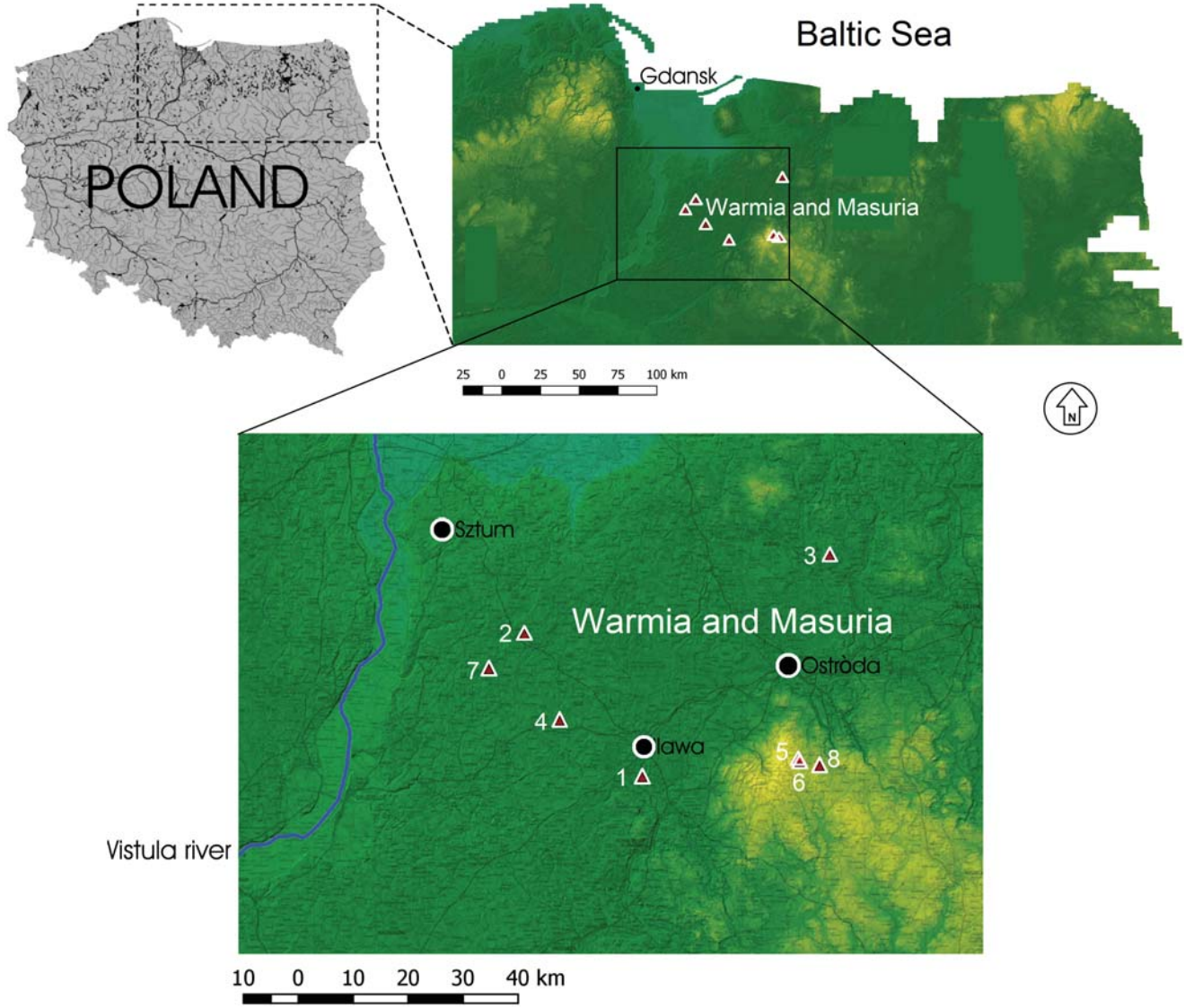

Fig. 1. Map of north-eastern Poland with location of selected Iron Age hillforts in Warmia and Masuria regions (triangles), based on ISOK, Geoportal: www.geoportal.gov.pl/en.

drawn on perfectly laid-out and oval-shaped hillforts dated to the Iron Age, which are surrounded by concentric moats and ramparts (Figs. 1–3). Despite the fact that some of these structures were already a subject of archaeological research, the available data still do not supply with sufficient information concerning their function (see Kobyliński (Ed.), 2017).

The prospection methodology of the hillfort on the Radomno Lake island (Fig. 4) is briefly presented below. Due to a dense forest cover, recognition of this archaeological site required application of integrated geoarchaeological prospection coupled with LiDAR and selected geophysical methods: ground-penetrating radar (GPR) and magnetometry. Prospection results were then imported to the GIS environment, which allowed planning of archaeological excavations in places guaranteeing acquisition of data for object dating and establishing its stratigraphy.

METHODOLOGY

ALS/LiDAR

Contrary to commonly accepted geophysical methods, which have been efficiently applied in non-invasive archaeological prospection for many years, ALS/LiDAR began to be commonly used for such purposes over 10 years ago, and the possibilities of its usage in archaeology are still open (see, Devereux *et al.,* 2005; Challis, 2006; Doneus *et al.,* 2008; Hesse, 2010; Doneus and Briese, 2011). Generally speaking, ALS is a remote sensing method based on measurement of a distance between the measuring device located on an aircraft and objects on a ground surface. A scanner with a range finder installed on the aircraft emits laser impulses with a given wave length. Impulses reflected from objects on the ground are registered by detectors. The

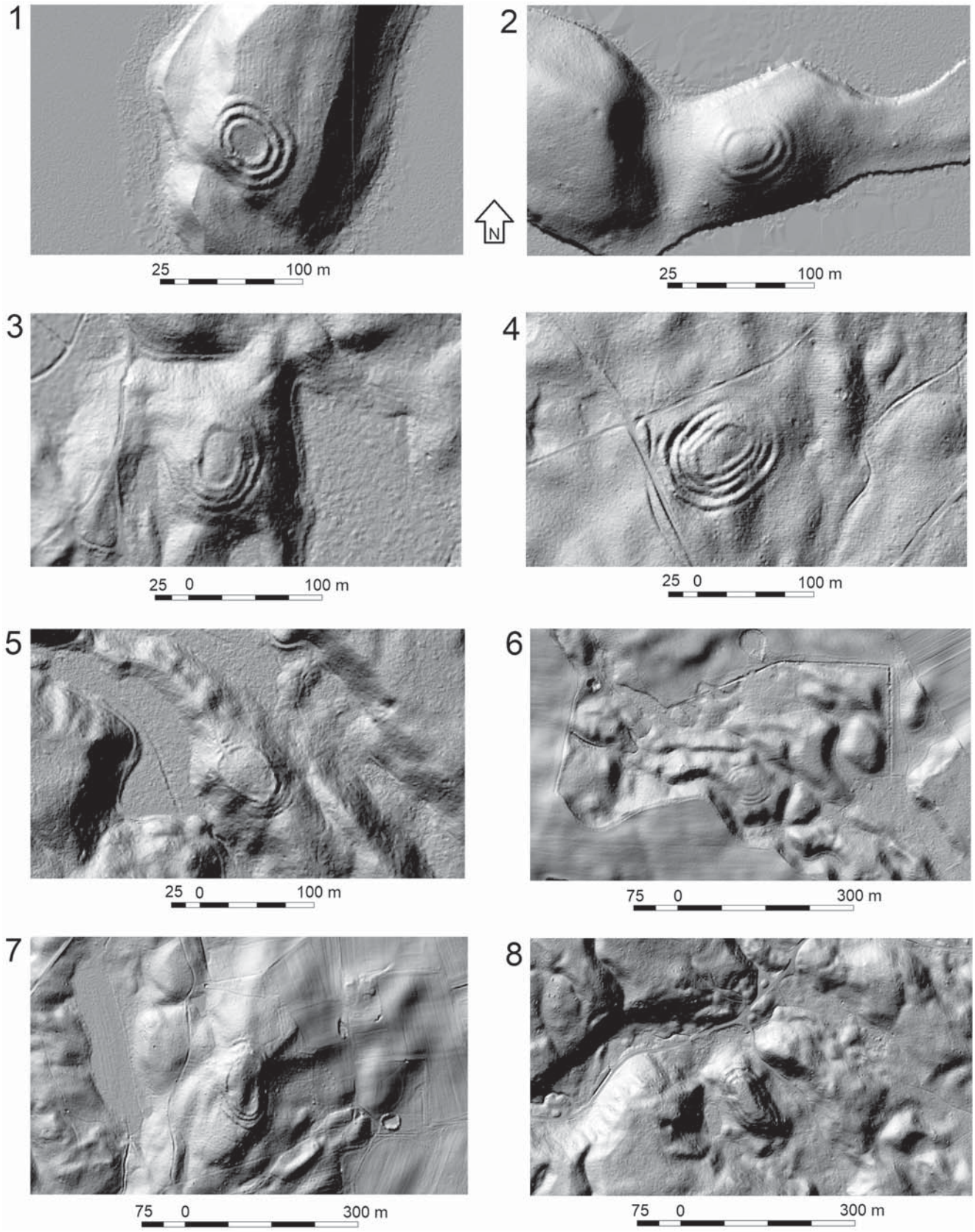

Fig. 2. Selected hillforts located in Warmia and Masuria regions on a LiDAR images, based on the ISOK-Geoportal resources (source: ISOK-Geoportal: www.geoportal.gov.pl/en). 1 – hillfort on the Radomno Lake island; 2 – hillfort on dense forested island of the Sowica Lake (near Prabuty town); 3 – hillfort in a forest near Tątławki village (see Kobyliński (Ed.), 2017); 4 – hillfort in a forest near Stary Folwark village (see Kobyliński (Ed.), 2017); 5 – hillfort in a forest near the Dylewskie Hills; 6 – hillfort in a forested area near Kitnowo village; 7 – hillfort in a forest near Gilwa village; 8 – hillfort in a forest on the Dylewskie Hills.

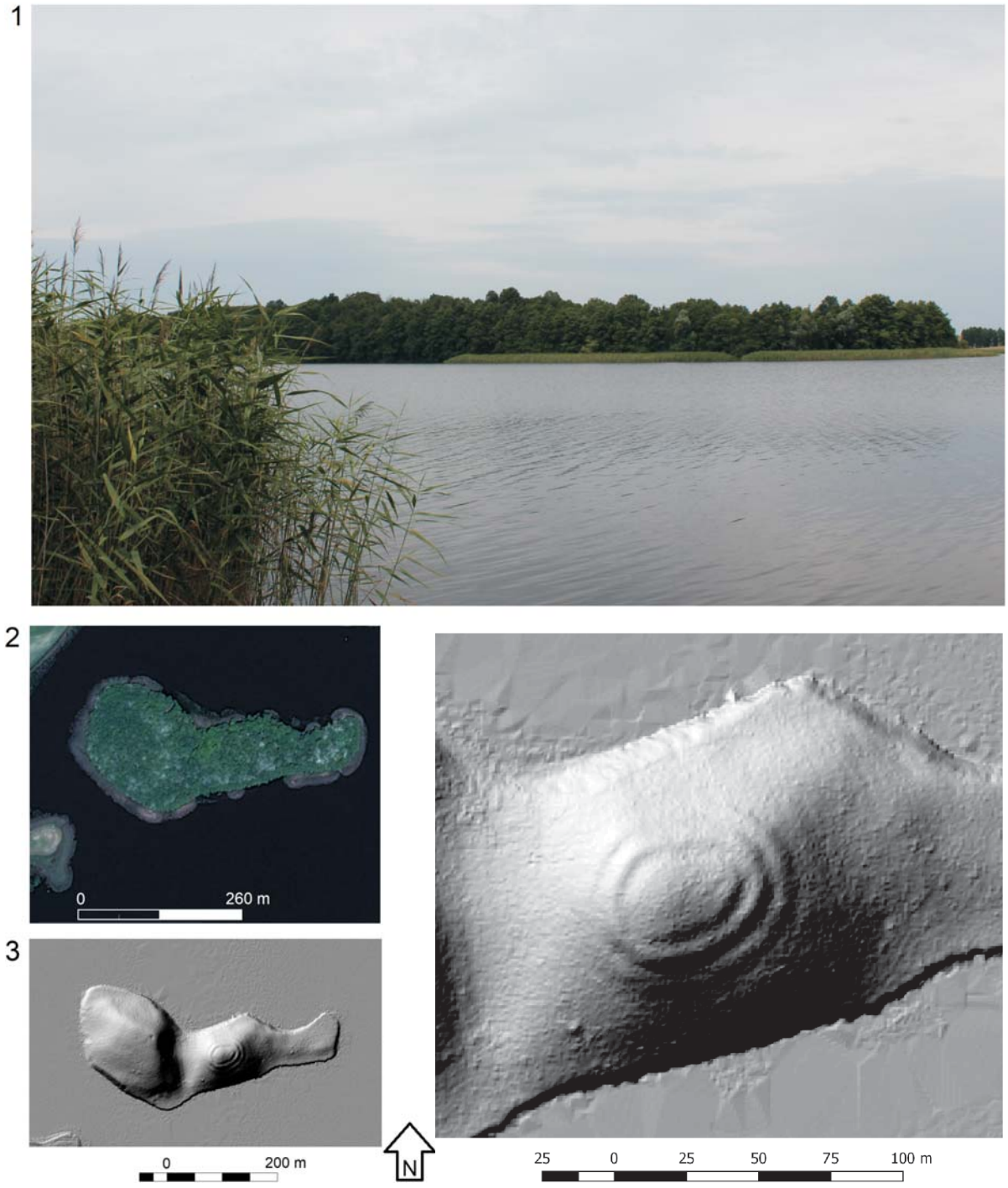

Fig. 3. 1 – general photo of the forested island on the Sowica Lake; 2 – aerial view of the island (Google Earth); 3 – LiDAR image (ISOK-Geoportal) of the hillfort preserved on the island.

airborne laser scanner is registering a rectangular zone transverse to the flight direction (see Ackermann, 1999; Wehr and Lohr, 1999; Challis, 2006; Crutchley and Crow, 2009). For the purpose of ISOK project in Standard I (4 points per 1 m^2), an impulse laser scanner was used. It works in near-infrared, usually at 1064 nm wavelength and with a velocity up to 500 kHz. Therefore, it was possible to register up to several tens of thousands points per 1 second (Kurczyński *et al*., 2015). The scanning unit operates in the GNSS and INS systems, due to which each registered laser reflection obtains its location described as coordinates X, Y, H in a specific datum (usually WGS-84). The obtained point cloud is a digital reflection of the scanned area. It should be pointed out that the ALS point cloud is encumbered with an error, particularly for the height value, which after averaging and depending on the scanning method lies in the range of ±5–15 cm (Crow *et al.,* 2008; Lasaponara *et al.,* 2011).

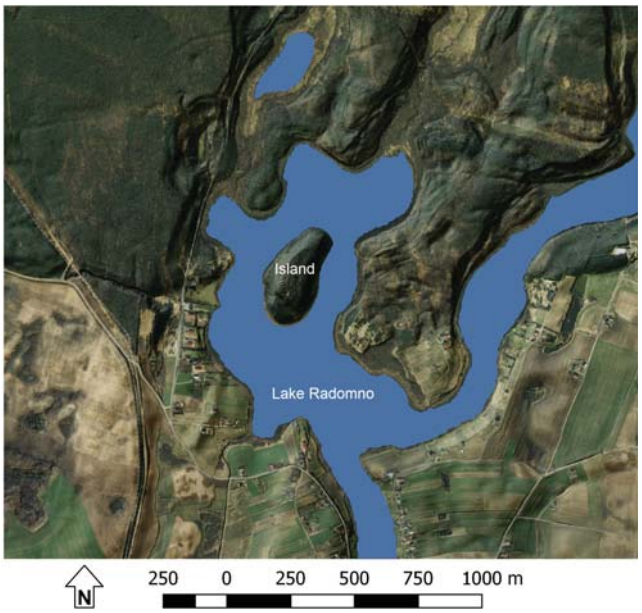

Fig. 4. Radomno Lake with a hillfort on the island visible on LiDAR image integrated with aerial photograph using QGIS software. Source of illustration: ISOK-Geoportal: http://www.geoportal.gov.pl/en.

In the ISOK data base, the point cloud is saved in the LAS format, which provides data on the position and number of subsequent reflections of each laser impulse. In the forested areas, a number of reflections may be high and they are a subject to specific classification (see Ducic *et al.,* 2006). Such form of data registration allows for constructing various models of the scanned area like digital surface model (DSM). Digital elevation model (DEM) requires filtering the ALS point cloud and removal of all reflections that are not classified to have come from the ground surface (Evans *et al.,* 2009; Doneus and Briese, 2011).

Location of archaeological objects and structures on ALS/LiDAR images is not an easy task, particularly with regard to forested areas. Pure interpretation of digital terrain models is not enough to determine whether a recognized object is of anthropogenic nature or not (Banaszek, 2014). Only some archaeological structures, such as settlements surrounded by ramparts and burial mounds, are characteristic enough to be interpreted easily and without a doubt. All other objects identified based on ALS models should be absolutely verified and a field recognition only allows to verify if the newly located object is not a group of bushes, a large boulder, fallen timber or a natural (geological) form, i.e. a small kame mound or kame terrace (Devereux *et al.,* 2005; Doneus *et al.,* 2008; Doneus and Briese, 2011; Banaszek, 2014).

Non-invasive field verification of archaeological objects discovered using ALS/LiDAR requires almost always application of geophysical methods. In forested areas of Warmia and Masuria application of magnetometry or GPR may be significantly hampered by a dense vegetation cover. The most difficult method to apply in such areas is electrical resistivity tomography, as it requires rearranging long electric lines and hammering the electrodes in a soil that is often densely overgrown with tree roots. For this reason, GPR and magnetometry were only applied for geophysical verification archaeological objects located during the project.

Ground-penetrating radar

The GPR is a mobile and highly effective method of the shallow subsurface geophysical prospection, which is based on emitting electromagnetic (EM) waves by a transmitting antenna and recording impulses by receiving antenna reflected from subsurface layers characterized by variable electrical properties. The range of GPR prospection depends on nominal frequency of a transmitting antenna and the electrical resistivity of the analysed geological medium. With decreasing frequency of the transmitting antenna the penetration depth increases; in this case, however, a resolution becomes lower. In turn, when the electrical resistivity of a soil is lower, then the depth range of a georadar is smaller, particularly in thick layers of mud, clay and silt (see, Owsin, 2009; Conyers, 2013, 2016, 2016a; Conyers and Leckebusch, 2010; Welc *et al.,* 2016, 2017, 2017a).

Correct calibration of a depth range on GPR images (reflection profiles) is a crucial issue in GPR surveys and it should be based on a knowledge about geology of a study area (Karczewski, 2007; Conyers, 2013, 2016). Because sand and silt prevail on the examined island (Gałązka, 2009) and measurements were done after rainfall, average velocity of electromagnetic wave propagation was accepted at 0.09 m/ns. Such value of velocity is noted for waves passing through e.g. dry, saturated sand, silt and clay.

The Groundexplorer HDR Ground-penetrating radar system produced by the Swedish company Mala/ABM was used during the survey on the island. A prospection was carried out with application of a shielded (bimodal) transmitting antenna with nominal frequency of emitted EM wave at 470 MHz. All obtained reflection profiles were processed using *ReflexW* (Sandmayer company) and *GPR Processes* and *GPR Slices* (prepared and published by L.B. Conyers) software with application of standard procedures such as running average, background removal filters, Dewow, DC – shift adjustments, manual gain adjustments and bandpass frequency filtering. In some profiles deconvolution, F-k filtration, migration and topographic correction processing were also applied. Finally, amplitude maps (depth or time slices) for different depths were created. During field measurements all profiles were separated from one another by 0.5 m.

Gradiometer

The second device used during non-invasive verification of archaeological objects in Warmia and Masuria was a Bartington Grad601 gradiometer (fluxgate type). It is one of the most effective methods at present used in non-inva-

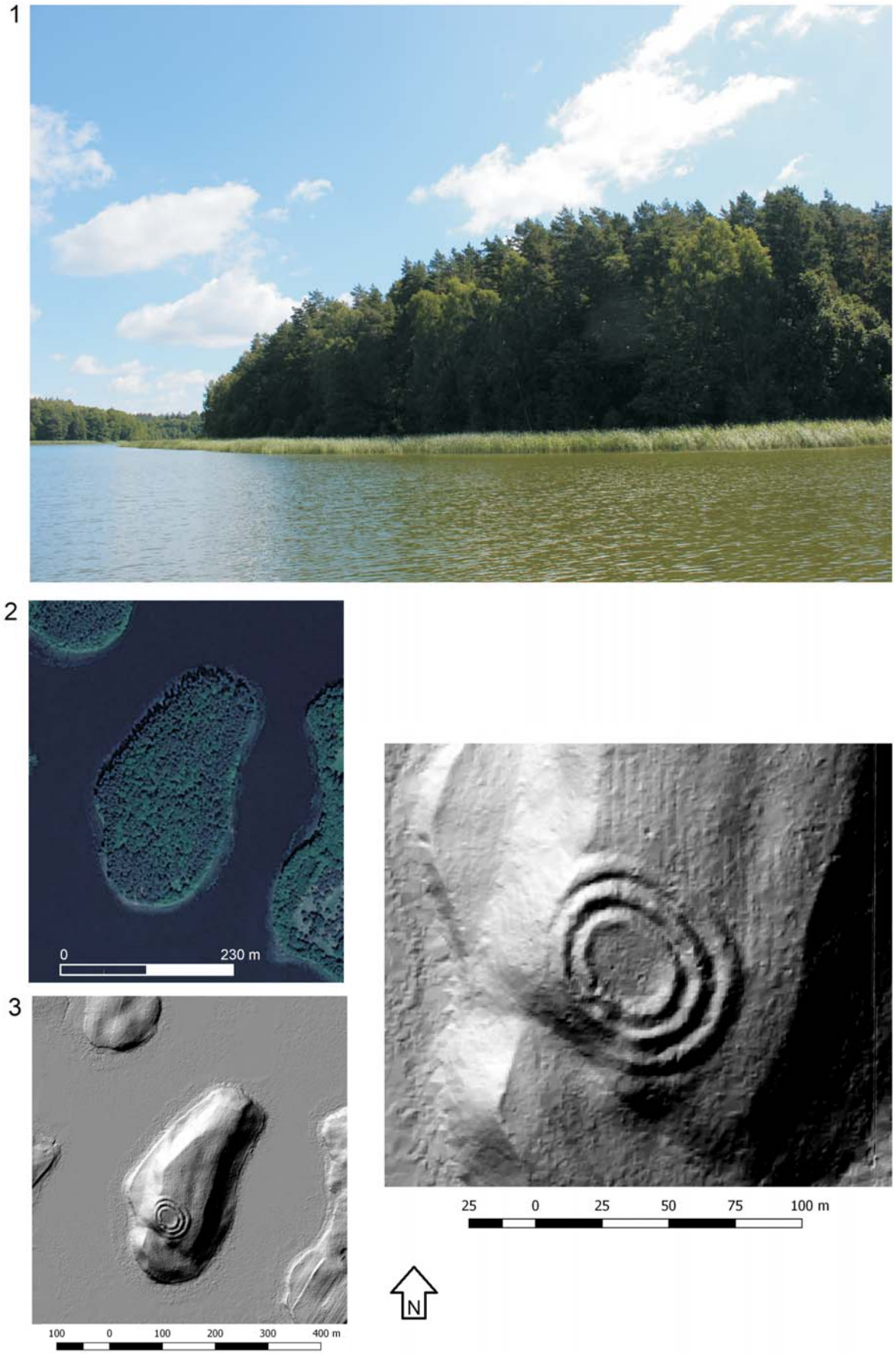

Fig. 5. 1 – general photo of the forested island on the Radomno Lake; 2 – aerial view of the island (Google Earth); 3 – LiDAR image (ISOK-Geoportal) of the hillfort on the island.

sive geoarchaeological surveys. The device does not register the entire magnetic field strength, but differences in values measured between two inductors assembled at different heights. The gradiometer thus measures differences in a field strength (vertical gradient) of the earth magnetic field. Therefore, objects close to the surface can be easily registered; at the same time disturbances related to changes in a geological structure or diurnal changes of the magnetic field strength, often very high, are avoided (Scollar *et al.,* 1990; Won and Huang, 2004; Aspinall *et al.,* 2008; Gaffney, 2008; Owsin, 2009; Fassbinder, 2015).

During magnetic survey on the Radomno Island measurements were done along parallel lines separated from each other at stable distance of 0.5 m. The measurement grids have been set to assure complete coverage of the hillfort surrounded by ramparts and moats, as well as of the adjacent area. Most polygons dimensions were 30×30 m and had identical orientation (Fig. 8). Presence of trees and bushes was a significant drawback during the survey, as a result of which some grids have smaller dimensions as well. The achieved prospection range may be estimated at about 0.5–1 m. All data were processed using *Terra Surveyor* software produced by the DW Consulting company (www.dwconsulting.nl).

Interpretation of geophysical anomalies on GPR images (depth slices and reflection profiles) or on magnetic maps are only an attempt to determine their real character and origin. Only excavations may fully confirm correctness of proposed interpretations. Therefore, both hand drillings and small archaeological trenches were done at the hillfort on the Radomno Lake island.

Fig. 6. View from the south-east (upper) and from the east (lower) on the ramparts surrounding a hillfort on the Radomno Lake island.

RESULTS OF INTEGRATED GEOARCHAEOLOGICAL SURVEY OF THE RADOMNO HILLFORT

ALS/LiDAR data analysis

Analysis of the DEM maps based on ALS/LiDAR data (available on Geoportal) allowed to determine location of several hillforts in Warmia and Masuria regions, surrounded by a characteristic system of three shallow moats and the same number of ramparts. All of them were located on hardly accessible hillocks and lake islands. They are mostly present in the central part of Warmia and Masuria regions (Figs. 1, 2). Some of them have been already verified and studied within another project (Kobyliński (Ed.), 2017, see also official web page of the project: www.grodziska-warmia-mazury.pl). Other hillforts, as the one located on the Sowica Lake island was located by F. Welc on LiDAR images and three other objects preserved in the area of the Dylewskie Hills were discovered for the first time following based on o LiDAR data analysis by Gałązka *et al.* (2015) (Figs. 2, 3).

One of the best preserved hillforts is located on the Radomno Lake island, several kilometres to the south of Iława (Fig. 4). The object is situated on an island located in middle part of the lake, whose present water level is at 90.2 m a.s.l. Morphology of the island is perfectly visible on LiDAR images, which indicate almost flat nearshore fragments, separated by steep slopes from the central, rather levelled peak of the island. A well preserved, oval-shaped hillfort is located in the highest point of the southern part of the island (c. 110 m a.s.l.). As it was mentioned, the island is built mainly of fine-grained, horizontally bedded kame sand and sandy silt. The shape of the island and its setting along a subglacial flow direction indicates that the form occurred at junction of 3 subglacial troughs (Figs. 5, 6) (Gałązka, 2009).

Analysis of LiDAR data supplied with many significant observations about morphology of the examined Radomno hillfort and the island itself. DEM images indicated an oval-shaped enclosure in a central part of the object (diameter of about 50 m) (Fig. 7: 1) and surrounded by perfectly preserved three ramparts, each about 10 m broad at a base and 1–1.5 m high. Ramparts are separated by shallow moats, about 1 m deep and several metres wide. A southern part of the object seems partly eroded (Fig. 7). This part has a distinct concavity in the rampart structure, suggesting presence of an entrance leading to the hillfort interior (Fig. 7: 2). Directly

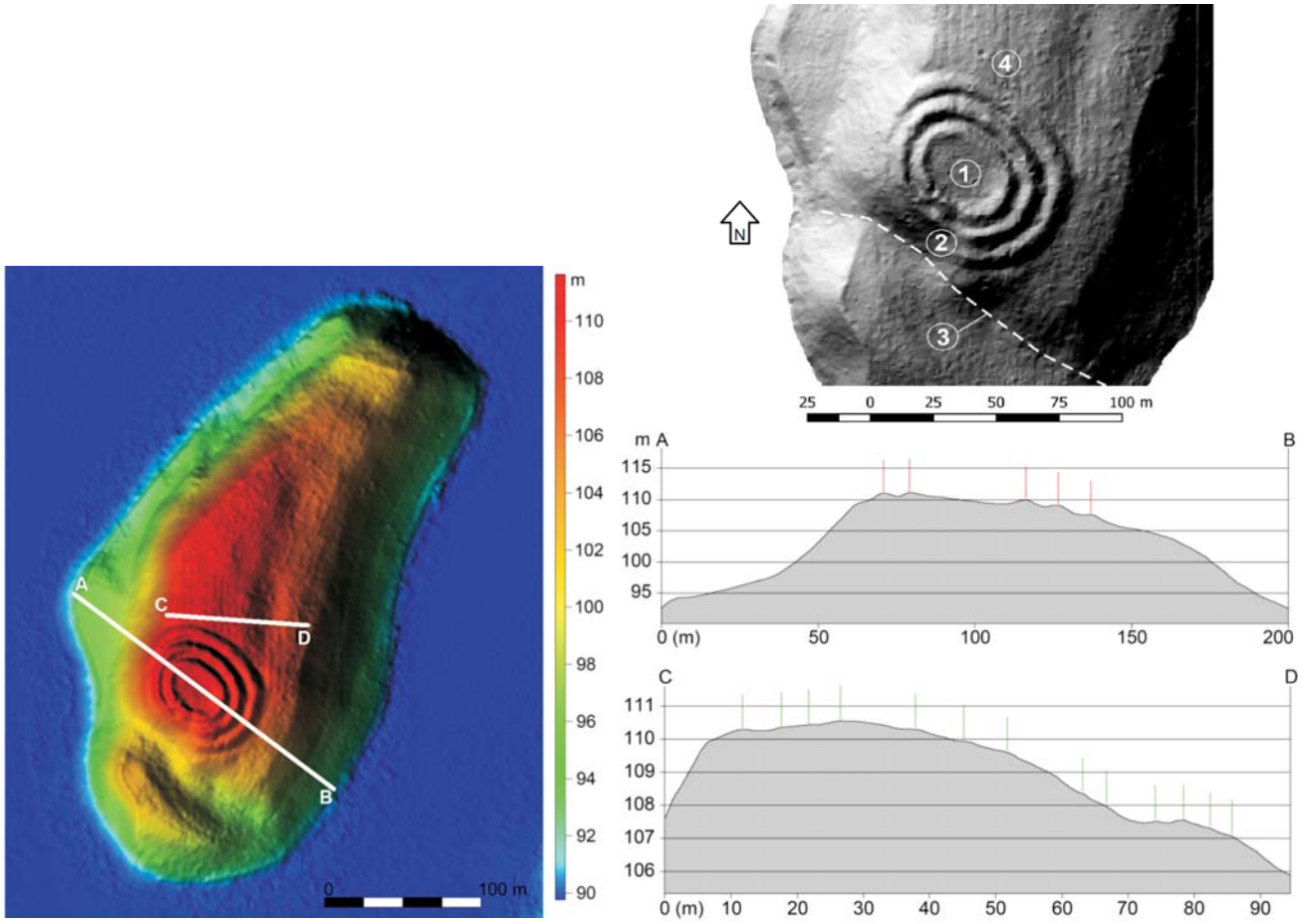

Fig. 7. LiDAR images of the hillfort preserved on the Radomno Lake island. 1 – oval-shaped, central part of object; 2 – system of ramparts and moats; 3 – undercut showing the landslide boundary, which caused destruction of the southern part of the hillfort; 4 – parallel linear structures preserved to the north of the object.

to the south of the object, there is a distinctive lineament: a steep, NW-SE oriented undercut which is most probably a massive landslide (Fig. 7: 3). It seems that presence of this feature is a reason for erosion of the southern part of the hillfort. Interestingly, directly to the north and north-east of the hillfort there are very clear, N-S oriented linear structures (Fig. 7: 4). They are low, parallel ridges, about 5 m wide and up to 50 m long, covering an area of about 0.5 ha. These structures are much less distinct on a narrow plateau located directly to the south-east of the hillfort.

Magnetometry

Geophysical survey carried out within the hillfort located on the Radomno Lake island significantly complemented the LiDAR data and brought new information concerning structure and stratigraphy of the hillfort (Fig. 8). The obtained so-called positive amplitude map of magnetic anomalies indicated presence of numerous high-amplitude zones (darker areas). Notable are anomalies with increased values of the magnetic field strength (0.8–1 nT/m), corresponding to a course of moats separating ramparts (Fig. 9). Significant increase of amplitude values should be linked with accumulation of organic matter and carbonized plant fragments in these depressions. Between the moats there are numerous smaller, mostly point high-amplitude anomalies. Some of them represent probably traces of past and current human activity, such as storage and dwelling pits, small fireplaces and also buried metal objects (characteristic dipole anomalies). Others are animal dens, deep holes and vast depressions created by tree roots, noted commonly during field prospection. In the case when dens are filled with sand, the map of magnetic anomalies reveals oval-shaped anomalies of small dimension (up to 1 m) and low amplitude (about 0.1 nT/m) (Fig. 9).

In the southern part of the Radomno hillfort, a zone of linear anomalies generated by moats and ramparts is not continuous, which may indicate presence of an entrance or gate leading to the central part of the object. Numerous point anomalies with variable amplitudes occur within the hillfort. These are both traces of past archaeological activities in the 20th century as well as numerous ancient settlement structures, most probably small storage pits filled with

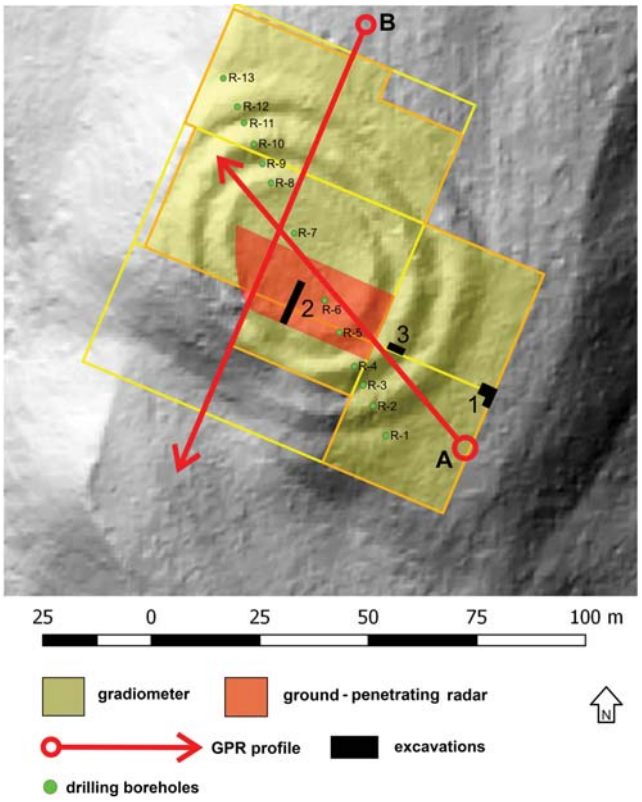

Fig. 8. LiDAR image of the hillfort preserved on the Radomno Lake island with boundaries of areas surveyed by magnetic and GPR techniques. There are also marked positions of performed geological drillings and archaeological excavations.

organic matter, ashes and pottery fragments. On the other hand, point dipole anomalies characterized by high amplitude corresponds to location of buried metal objects (Fig. 9).

Poorly visible outline of a circle, about 30 m in diameter, can be noted in their somewhat random pattern inside the Radomno hillfort. The circle has an asymmetric position, i.e. in the southern part of the inner oval-shaped area of the hillfort (Fig. 10: A). Linear structure emerges also in the circle; however, it is difficult to interpret based on magnetic plan only due to large number of high-amplitude dipole anomalies. In order to recognize local stratigraphy and nature of registered anomalies in the inner, southern part of the hillfort, a trial trench (oriented on the N-S axis) was excavated (see Figs. 8: 2; 10: B). It revealed a burnt wooden wall at of ca. 0.70 m depth, composed of two parallel beams oriented north-south (Fig. 10: B).

The map of magnetic anomalies of the area directly in the north of the hillfort reveals parallel linear, N-S-oriented structures, which are perfectly visible on LiDAR images (Fig. 9). The zone of linear and point anomalies is also present directly to the east of the most external moat, partly destroyed in this place, which may suggest that the anomalies are generated by objects and structures that are chronologically later with regard to the hillfort (Fig. 11). An outline of a dwelling structure erected on a plan close to a rectangle with an internal oval object may be observed there. A small trial trench excavated in this place (Fig. 11: A) confirmed presence (at ca. 0.6 m depth) of a poorly preserved dwelling structure with oval and shallow pit inside. The AMS radiocarbon date from the sediment in the interior of a pit pointed out to 1445–1632 cal. AD (95.4% probability) i.e. late Middle Ages (Fig. 11: B). The map of magnetic anomalies produced

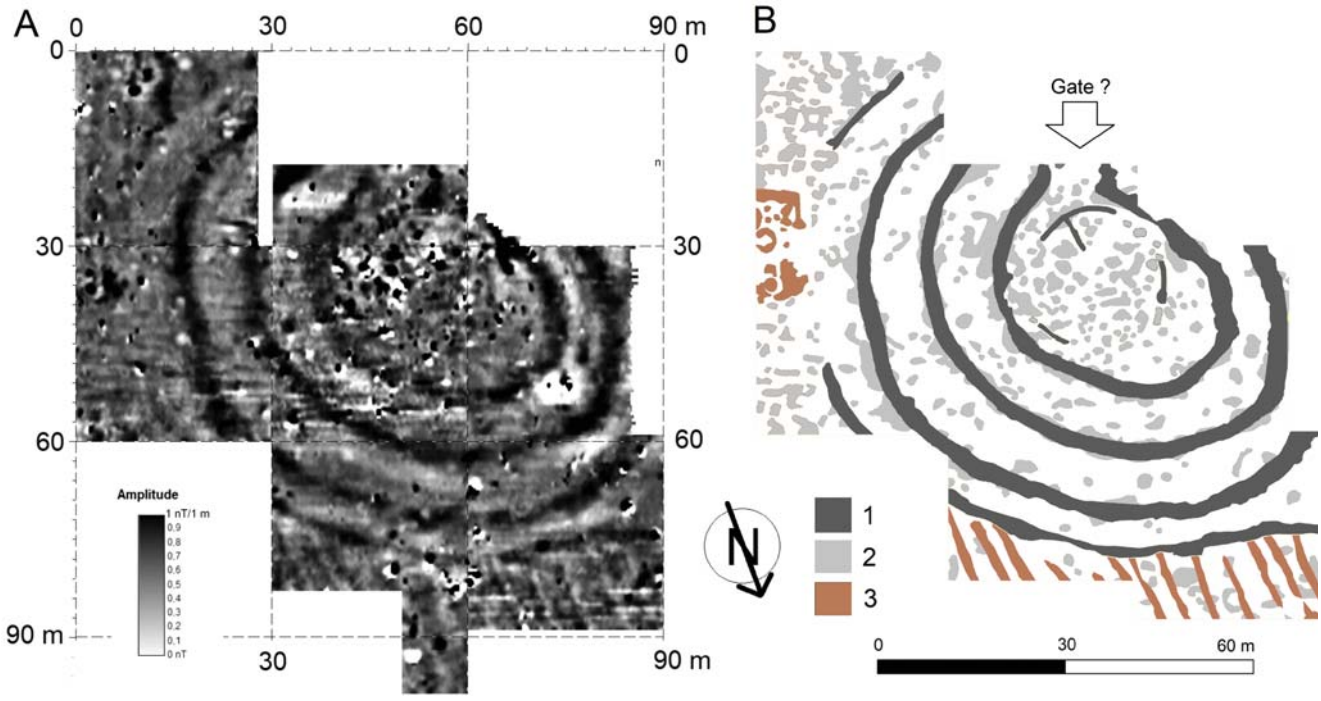

Fig. 9. Results of magnetic prospection (gradiometer) conducted at the Radomno hillfort presented as the amplitude map (see detailed explanation in text). Interpretation: 1 – outlines of moats separating ramparts; 2 – point source anomalies (traces of past and modern human activity); 3 – remains of the past settlement structure and linear features preserved to north of a hillfort.

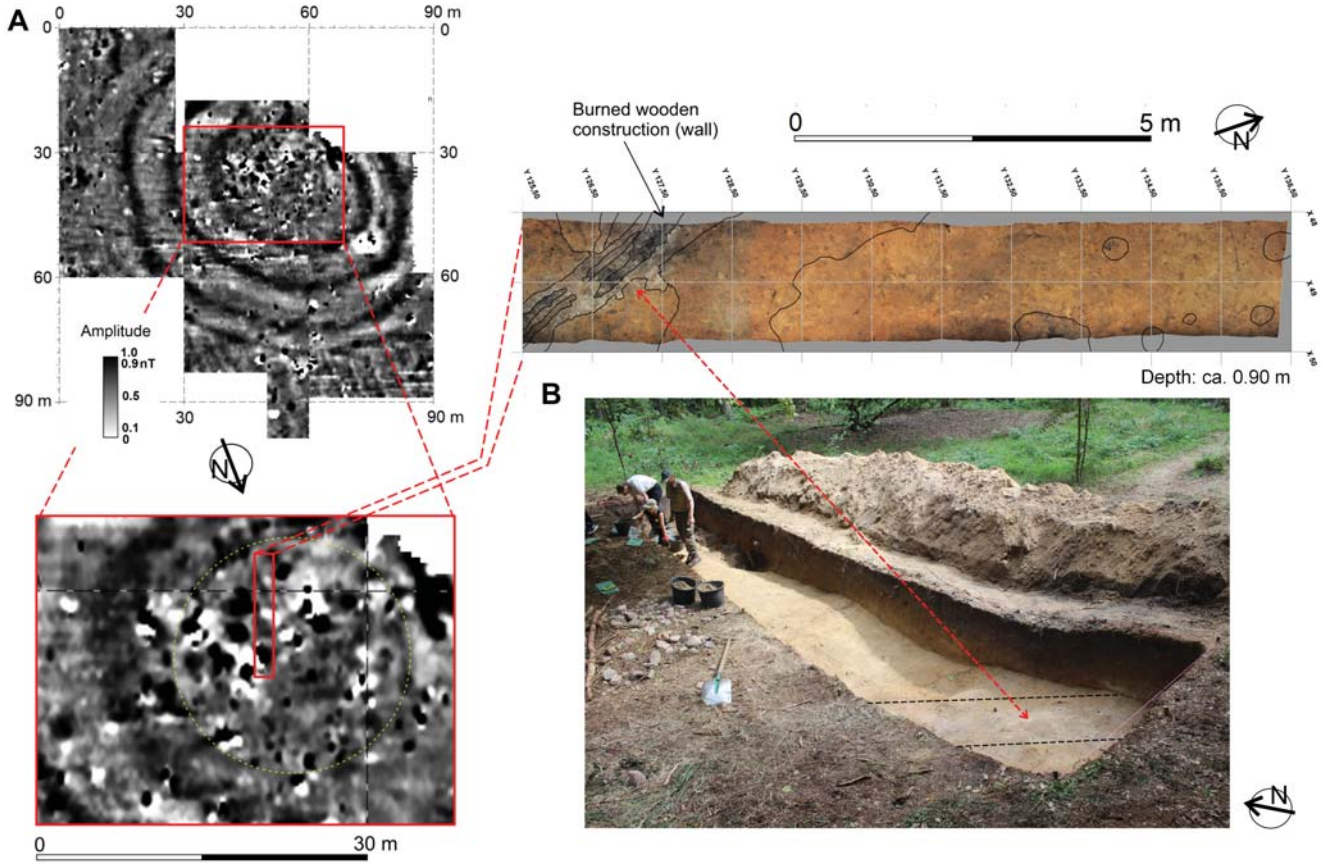

Fig. 10. A – results of magnetic prospection showing outline of a circle inside of the Radomno hillfort; B – excavations conducted inside of a hillfort revealed (ca. 0.5 m depth) burnt wooden wall composed of two parallel beams oriented north-south.

for the area directly adjacent to the hillfort from the north also reveals parallel linear, N-S-oriented structures, which are perfectly visible on LiDAR images (Fig. 11: C).

GPR

Due to dense vegetation, only the areas devoid of trees and bushes were surveyed with the GPR method. Moreover, long and single profiles were also done to receive additional data on geology of the island and stratigraphy of the hillfort. In order to enhance understanding of georadar profiles, assemblages of basic anomalies visible on reflection profiles, determined as GPR facies, are shortly characterized below:

– zone without anomalies, indicating strong signal attenuation of EM (mud, silt and clay),
– diffraction hyperboles: characteristic arcs visible on GPR reflection profiles generated by buried anthropogenic objects, stones, large boulders or rock fragments,
– horizontal lines reflecting boundaries between two layers,
– multiplied horizontal lines reflect multiple returns from the boundary between two layers or geological media (see Welc *et al.,* 2016).

The most interesting results came from GPR prospection made in a central part of the hillfort (see Fig. 8). The obtained GPR amplitude maps (= depth slices) have revealed a series of linear anomalies at about 0.50 to c. 0.70 m depth. They are produced by remains of an unidentified feature with rectangular outline and SW-NE orientation (Fig. 12). In turn, the circle outline, recognised on the map of magnetic anomalies, is very poorly visible at 0.35–0.45 m depth. Analysis of selected reflection profiles supplied with additional information on stratigraphy of the central part of the hillfort. All profiles reflect a distinct stratigraphic horizon visible as discontinuous horizontal reflection surface at about 0.70 m depth (Fig. 13, red line). Above this boundary there are numerous diffraction hyperboles, which evidently may be linked to past human activity. They are mostly generated by large stones and another buried objects. Noteworthy are also small depressions, which are most likely ancient storage pits (Fig. 13). Results of 3 shallow drillings (R 5–8) in the central, oval-shaped part of the hillfort revealed the following sedimentary succession (Fig. 8): 0.0–0.2 m – dark grey sandy soil, 0.2–0.6 m – grey and brown-grey fine sand, 0.6–0.7 m – yellow-brown medium-grained sand (top of undisturbed soil) and 0.7–2.0 m – yellow-grey sand with silt. Drillings

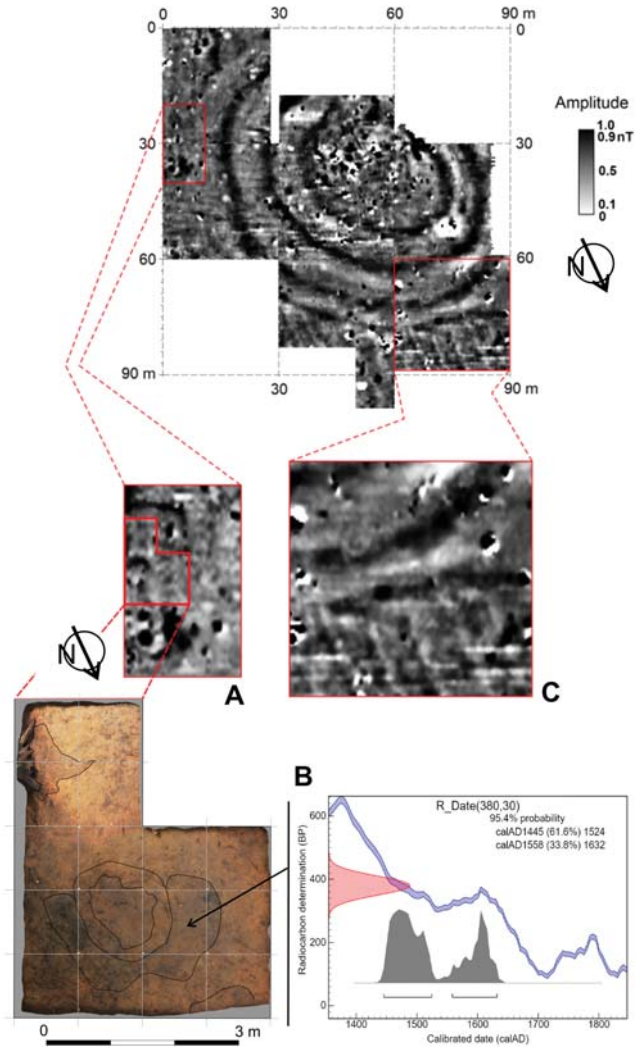

Fig. 11. A – results of magnetic prospection and excavations showing outline of poorly preserved dwelling structure with an oval and shallow pit inside; B – AMS radiocarbon date of a sample collected in the interior of a pit; C – fragment of a magnetic map revealing linear structures in the area directly adjacent to the hillfort from the north.

indicate that the cultural layer in the central part of the object is about 0.5 m thick, which may be perfectly correlated with GPR measurements. At 0.7 m depth the reflection surfaces separate anthropogenic sediments (cultural layers), i.e. grey and grey-brown sand with high content of organic matter and iron oxides, from the well-sorted, yellow kame sand and silt. Large number of discontinuous reflective surfaces below 1.0 m on analysed GPR reflection profiles indicates a more variable lithological structure of the basement, most probably due to presence of fine gravel and coarse sand interbeds (zones of signal amplification) and silt (zones of attenuation of electromagnetic waves) (Fig. 13). These structures should be associated with presence of ancient fluvial channels, most probably activated within a glacial kame in the Late Pleistocene. Flows took place in ice lumps that covered a kame reservoir. In the upper part the channel is filled with fine gravel and poorly sorted sand, in the lower one there are mostly sand and silt (Fig. 14).

For a full recognition of the object stratigraphy two long GPR profiles were performed along the longer and shorter axis of the hillfort with application of topographic correction (terrain morphology). The profiles covered both the object and the foot of the hillock, on which it is located (from the south-east) (see Fig. 8). Within the hillfort, the profile A has similar stratigraphy as the one described above. At about 0.7 m there is a distinct reflective surface separating anthropogenic accumulations (Fig. 15: A, 1) from geological layers (Fig. 15: A, 2), in this case sands interbedded with silt and gravel. At 1.5 m depth there are at least two fluvioglacial channels in kame deposits (Fig. 15: A, 3).

The profile A provides important information about the hillfort stratigraphy. A rampart structure is clearly visible. The close-up of the profile in this particular place indicates two distinctive reflection surfaces generated by the rampart base (palaeosoil). It proves that ramparts were created using the sediment taken directly from the moats (Fig. 15: B, 3 and 13). What is more, concentration of diffraction hyperbolas above a palaeosoil suggests that there was a wall or a wooden palisade (Fig. 15: B, 27). These assumptions were fully confirmed by the archaeological trench no. 3 located on the middle rampart (eastern section) (Figs. 8 and 15: B). Remains of the wooden wall were revealed there, very similar to the wall discovered in the central part of the hillfort (see Fig. 10). Radiocarbon date obtained from a sample taken from the foundation of the middle rampart dates its construction to the Middle Roman Period (128–258 cal. AD, 95.4% probability) (Fig. 15: B).

The GPR profile B presents a similar stratigraphy as in the profile A (Fig. 16). At about 0.7 m depth a distinct reflection surface occurs which separates anthropogenic (Fig. 16: 1) and geological layers (Fig. 16: 2). At 2 m depth the profile reveals the next horizontal reflection surface which is generated by already described bottom of a fluvial channel formed inside the kame structure (Fig. 16: 3). Fragment of the profile with a foot of the hillock supplies with interesting data concerning destruction of a southern fragment of the hillfort (Fig. 16: 4). By application of a topographic correction it was possible to determine the actual dip of layers that build the hillock. This is of crucial significance, because lack of topographic correction in the case of surveys in areas with variable topography does not allow for a correct interpretation of GPR profiles. This results from the fact that during surveys running across depressions, e.g. ditches, the electromagnetic waves are reflected from their sides and then registered on GPR reflection profiles. Moreover, reverberations between the antenna and the ditch bottom overlap, which results in anomalies on GPR images that are very difficult to interpret (see Conyers, 2013). A fragment of the long GPR profile running across the hillock reveals an almost vertical boundary between slope layers of its southern margin and its foot. Lack of continuity between the slope layers and those forming the hillock foot suggests that in reality this boundary is a slip surface of a landslide, which caused

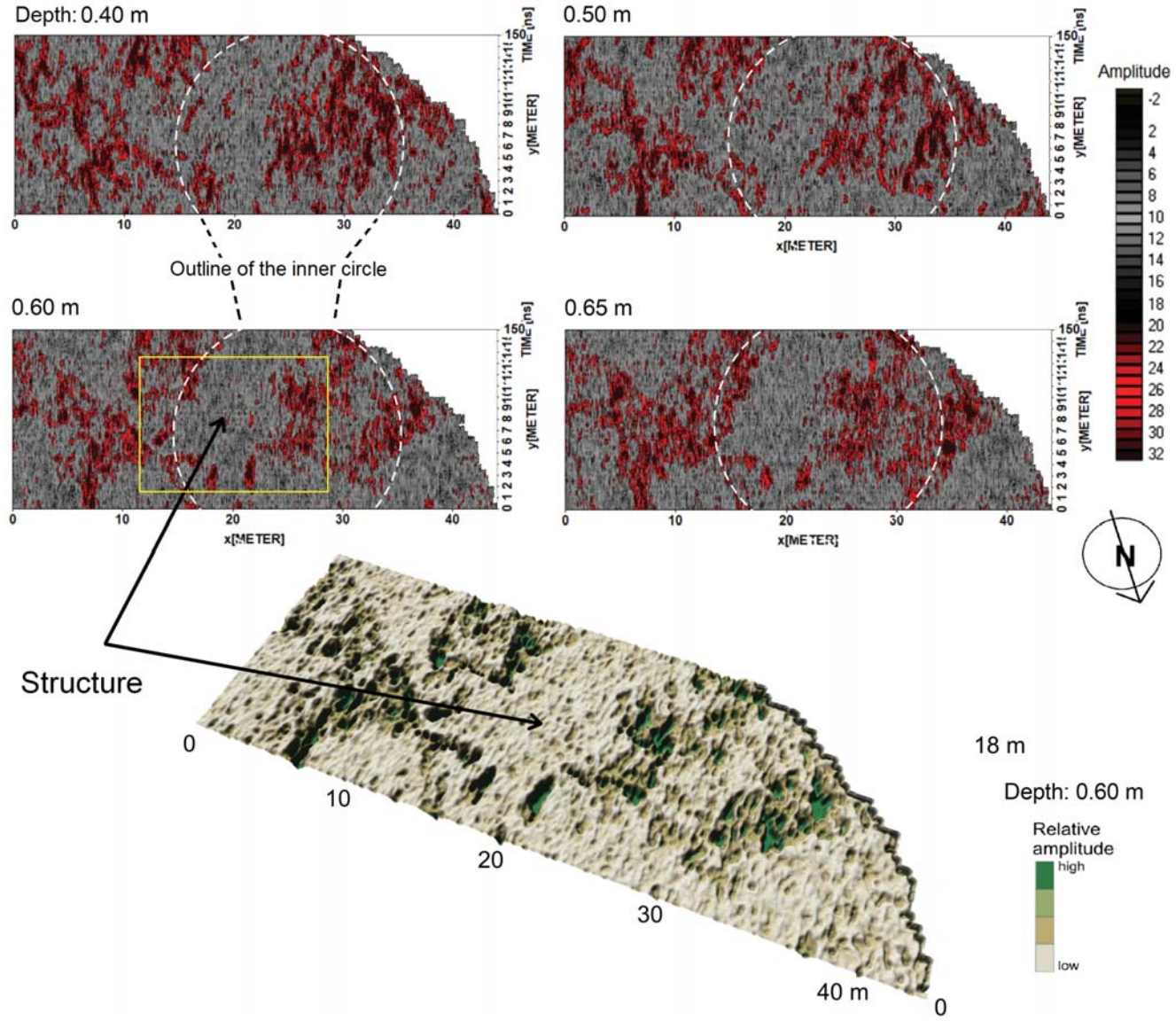

Fig. 12. Results of GPR prospection conducted inside of the Radomno hillfort (see explanation in text) in the form of the time slices prepared for selected depth intervals. They revealed a series of linear anomalies at 0.5–0.7 m depth, produced by remains of an non-defined archaeological feature with rectangular outline and SW-NE orientation.

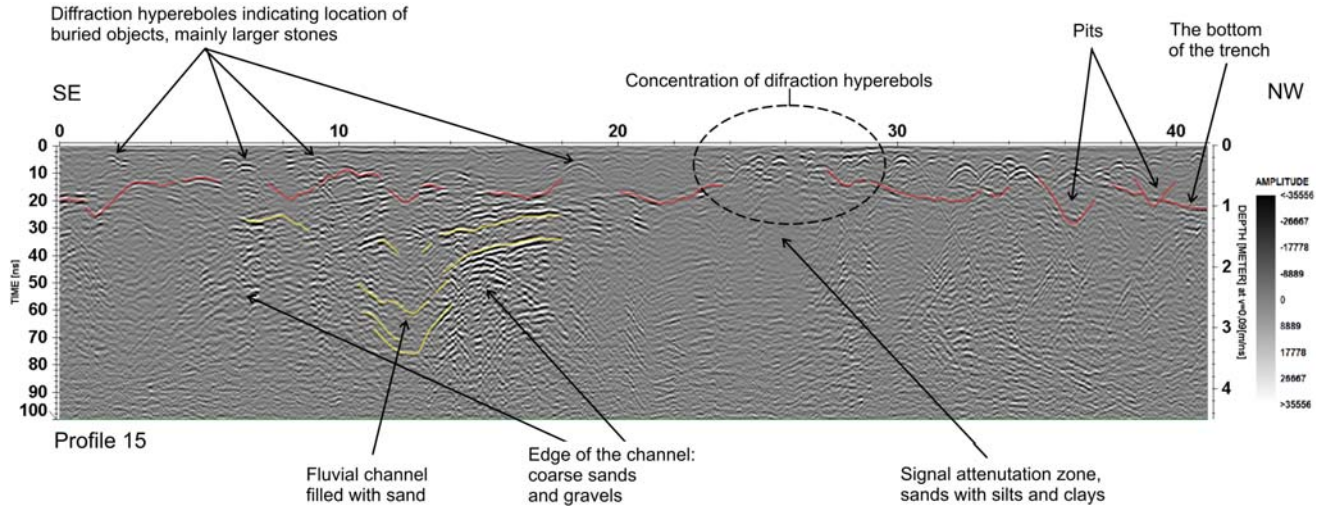

Fig. 13. Interpretation of the GPR reflection profile no. 15 in a central part of the Radomno hillfort.

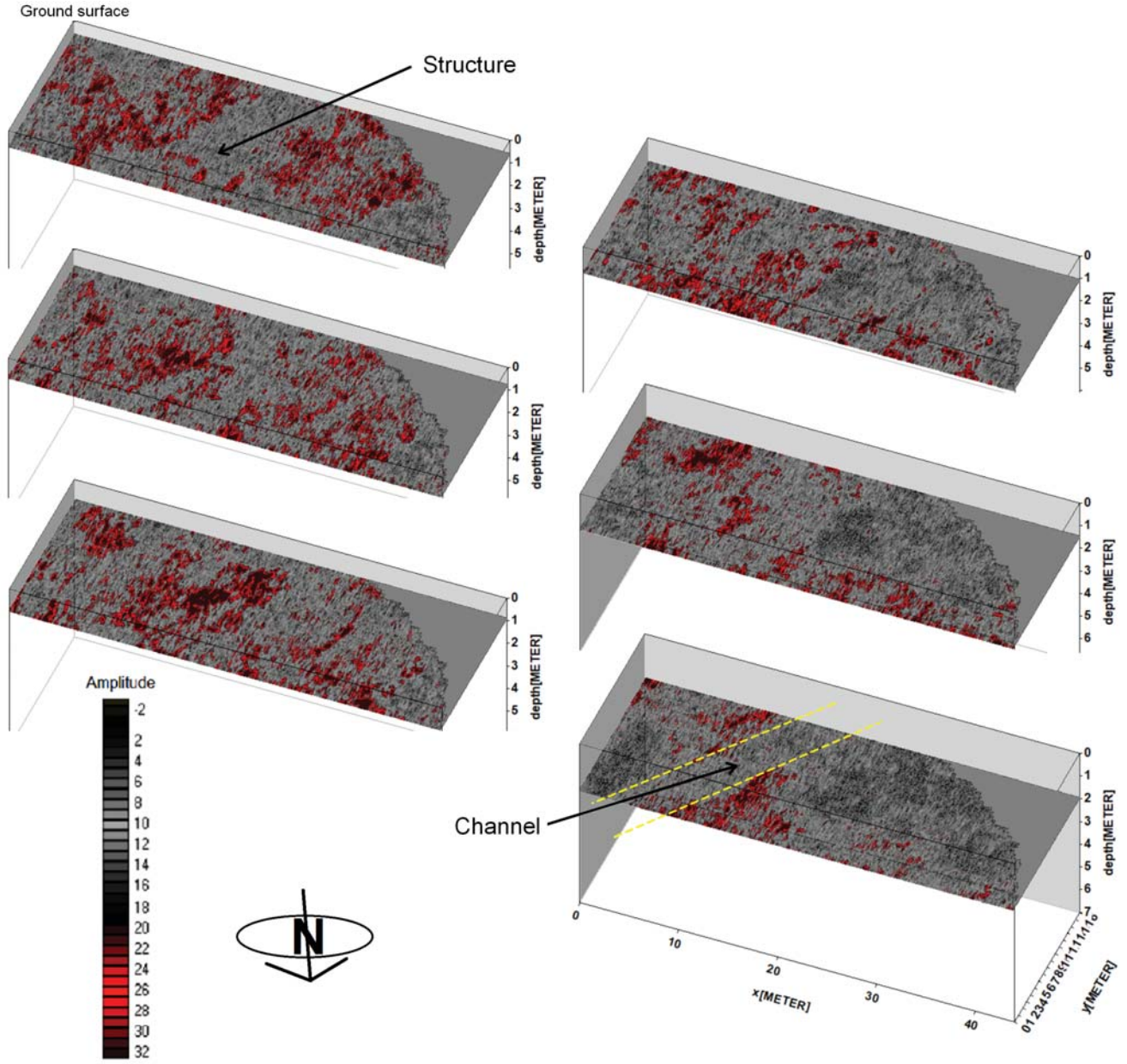

Fig. 14. Results of GPR prospection conducted inside the Radomno hillfort in a form of time slices (quasi 3D mode). Presented planes revealed a series of linear anomalies at 0.5–2.0 m depth m, generated both by anthropological and geological features (see explanation in text).

destruction of the southern part of the hillfort (Fig. 16: 4). Such supposition is confirmed by the hillock morphology reflected in LiDAR images (see Fig. 7: 3). If this interpretation is correct, then the landslide must have been formed sometime after the construction of the Radomno hillfort.

DISCUSSION AN FINAL CONCLUSIONS

Analysis of public LiDAR data acquired from CODGiK allowed location of similar Iron Age hillforts, surrounded by a characteristic system of moats and ramparts preserved on hardly accessible hillocks and islands of the Warmia and Masuria regions (north-eastern Poland). These objects are quite unique, not only because of their shape but also due to excellent proportions, layout and state of preservation. Integrated geoarchaeological survey of such hillfort, preserved on the forested island of the Radomno Lake indicated benefits of using digital elevation models (DEM) that can be correlated with results of geophysical surveys and shallow drillings. In effect, not only form and structure of objects can be recognized, but also their geology and stratigraphy. Analysis of DEM images indicated that an oval-shaped enclosure with about 50 m diameter, surrounded by three ramparts separated by shallow moats preserved on the top of the Radomno Lake island. To the south of the structure there is a NW-SE oriented undercut, which developed probably due to a massive landslide. This landslide

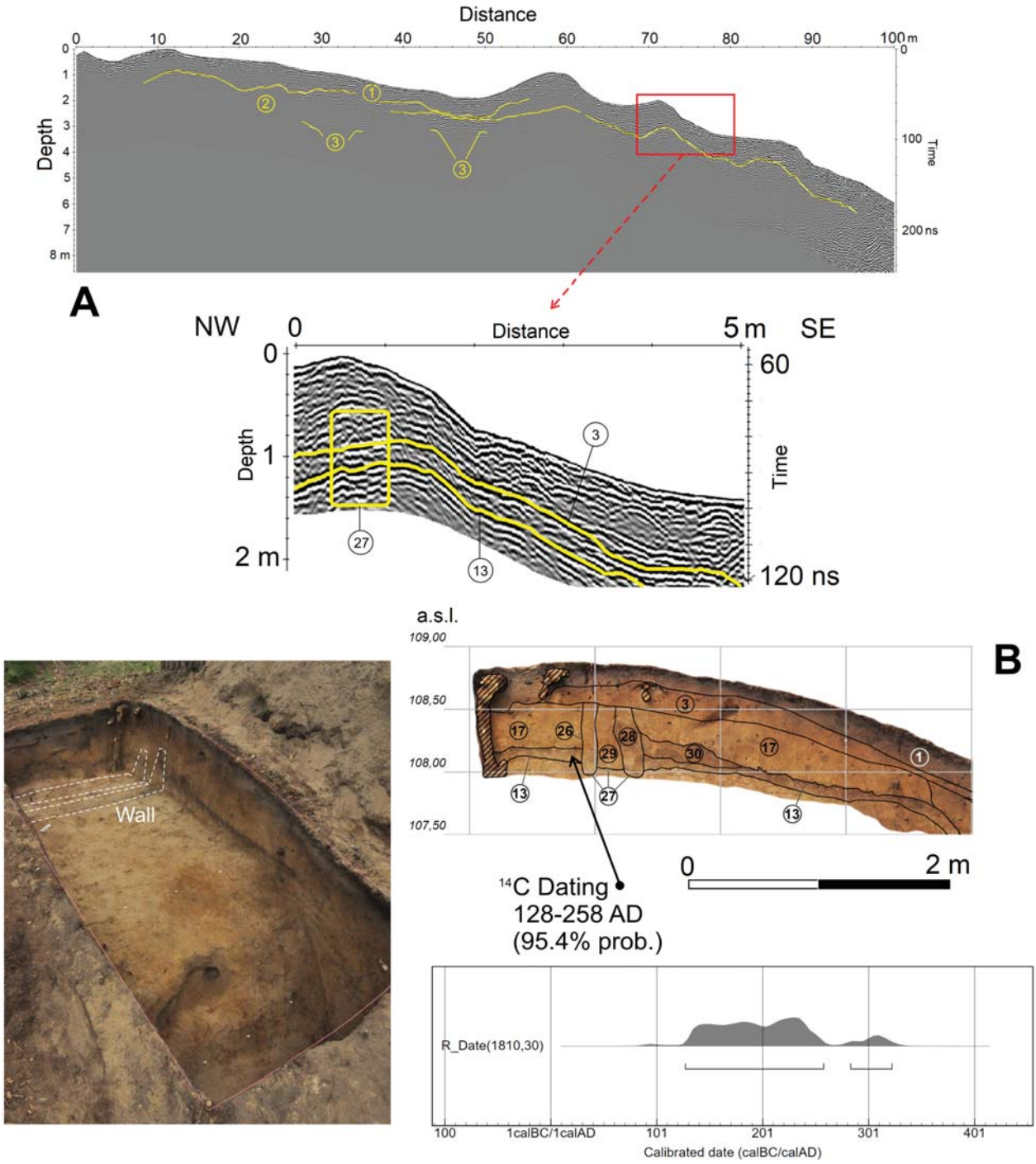

Fig. 15. A – long GPR reflection profile intersecting the Radomno hillfort (on the SE-NW axis) presenting geological structure and archaeological stratigraphy of the object (see explanation in text); B – results of excavations (with numbers of most important stratigraphic units) made on the middle rampart of a hillfort and result of radiocarbon dating of a sample collected at the base of the embankment.

caused most probably a partial destruction of the hillfort. A concavity in the rampart structure in the southern part of the object may point out to presence of the main entrance leading to its central part. Similarly as LiDAR images, results of magnetic prospection indicated that the main entrance was probably located in the southern part of the object. A magnetic map revealed a large number of amplitude anomalies in a central part of the hillfort. The outline of a circle, 30 m in diameter, with linear structures in its interior, was recognized there and fully confirmed by excavations. In their course a fragment of burned wooden wall was found. To the east of the most external rampart there were concentrations of numerous magnetic anomalies generated by archaeological objects and structures, most

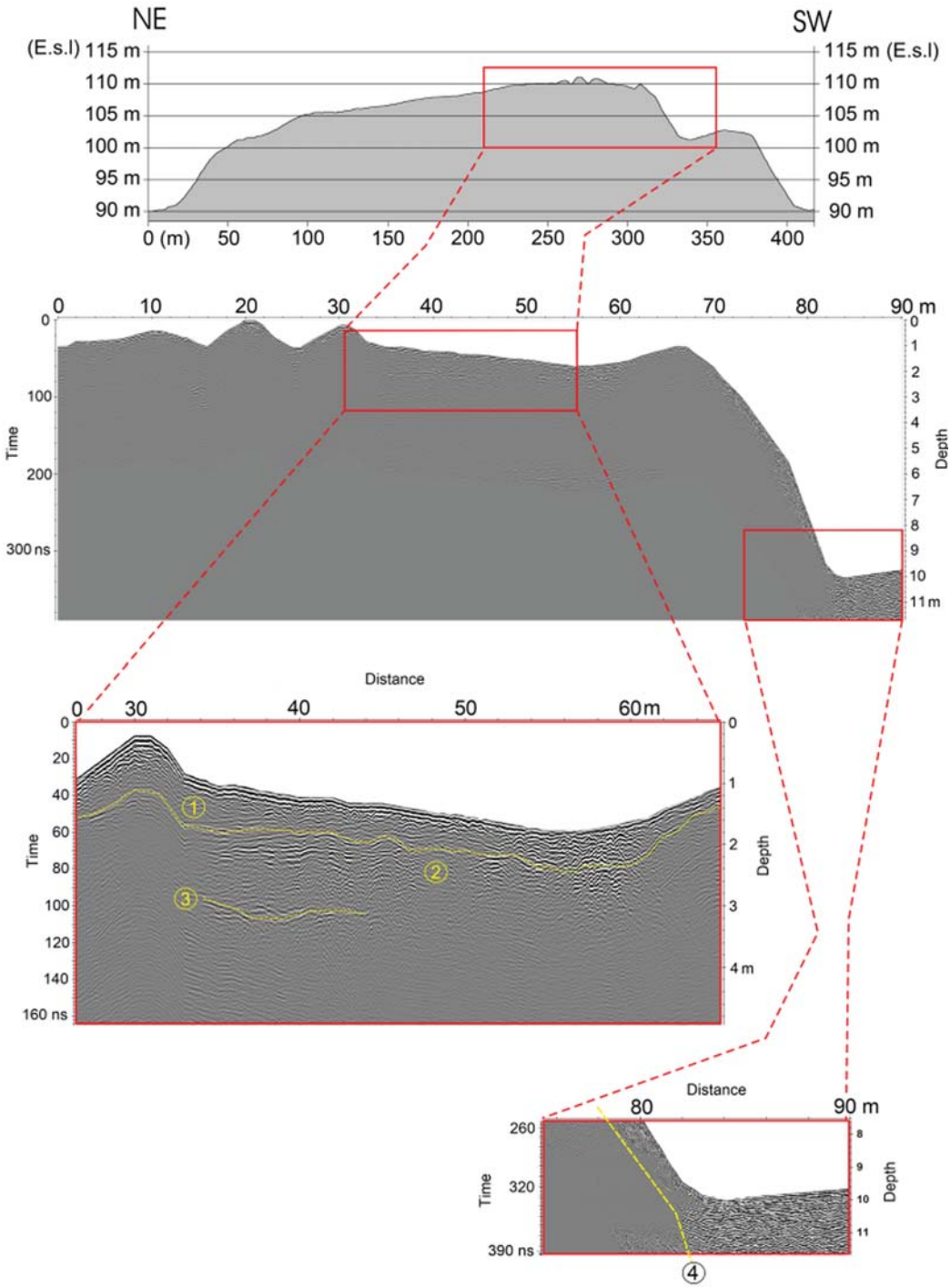

Fig. 16. Long GPR reflection profile marked as B across the Radomno hillfort (on the NE-SW axis) revealing its geological structure. 1 – distinct reflection surface which separates anthropogenic sediments from geological layers (2); 3 – horizontal reflection surface which is generated by bottom of the fluvial channel formed inside the kame structure; 4 – fragment of the profile with the foot of the hillock revealing slip surface of a landslide, which caused destruction of the southern part of the hillfort.

probably related to past settlement activities. Also here, the excavations confirmed presence of a dwelling structure dating back to the late Middle Ages (Fig. 17).

Results of the GPR prospection conducted within the hillfort supplemented significantly magnetic and LiDAR data. Differences between two methods of geophysical prospection are significant. The concentration of ferromagnetic minerals, such as destruction layers, concentration of ashes, firing places, furnaces, trenches and fired brick foundation can be mostly traced on maps of magnetic anomalies. But not all of them are visible on the interpreted GPR depth slices and reflection profiles. On the contrary,

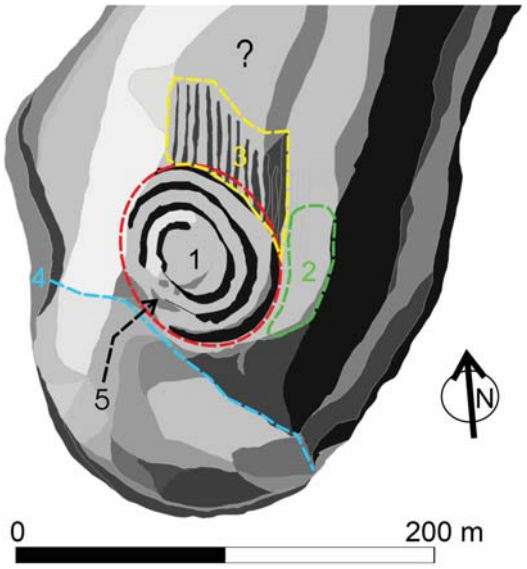

Fig. 17. Sketch-map of the southern part of the Radomno Lake island. 1 – Iron Age hillfort surrounded by a system of three ramparts separated by shallow moats; 2 – area with traces of settlement structures; 3 – enigmatic N-S-oriented linear structures (ridge and furrow structures?); 4 – boundary of landslide, which caused destruction of the southern part of the object; 5 – probable entrance.

magnetic data do not deliver information about depth and vertical cross-sections of recognized anomalies supplied by GPR. Reflections traced by GPR are produced by real (physical) remains of underground structures, buried objects or a contrast between layers with very different electric properties (Conyers, 2018). GPR prospection in the central part of the Radomno hillfort revealed a series of NE and NW-oriented linear anomalies, most probably generated by archaeological structures. Application of topographic correction allowed to get the GPR cross-section, not only through the structure of the object but also through a southern part of the hillock slope. A contact between the layers at its foot suggests that this is an undercut surface of an old landslide, which contributed most probably to destruction of the southern part of the hill and southern fragment of the hillfort encompassing two external ramparts.

Maps of magnetic anomalies and LiDAR images indicated characteristic N-S oriented linear structures in the area adjacent to the hillfort from the north and north-east. The most crucial issues are their age and function. The contact of these ditches with the external system of hillfort ramparts indicates that they are younger than the object. The nearest analogies are the traces that are formed due to ridge-and-furrow cultivation. In England this technique was used till the end of the Middle Ages (McOmish, 2011). In Central Europe this technique was documented also in Denmark (Lewis, 1999). In Poland this kind of field system is known for example from Borysławka (Affek, 2016). Dating these traces to the Middle Ages confirms presence of a structure from this period that was discovered to the east of the Radomno hillfort. It should be considered whether the island with its hillfort was not used as a refugium during the Middle Ages. Thus, traces of cultivation would be relics of short-term cultivation in a part of the island by people that took refuge in the settlement. This interpretation is also confirmed by Middle Ages ceramic fragments on the island.

Several fragments of thick-walled pottery with roughened outer surface, characteristic for the Early Iron Age phase of the Western Balt Barrow Culture were discovered during excavations and surveys conducted by the authors on the Radomno Lake island. This material allowed to date the initial construction of the hillfort at the Early Iron Age. This assumption seems to be confirmed by results of earlier archaeological verification carried out on the island in 2011. Nine small trial trenches (to 1 m depth) were dug at that time in a central part of the hillfort and inside ramparts and moats (Gręża wski, 2013). The mentioned radiocarbon date (128–258 cal. AD, see Fig. 15: B) from the base of the middle (palaeosoil) rampart suggests that the hillfort was used at least in two phases. It was built most probably in the Early Iron Age (c. 2–3th century BC). At the turn of 2nd and 3rd century AD the rampart system was again raised (renovated) and in the same time the ditches were deepened. This explains relatively good state of preservation of the Radomno hillfort compared to similar objects presented in this paper, such as Tątławki hillfort, Stary Folwark hillfort or the object on the Sowica Lake island (see Fig. 2). It does not change the fact that confirmation of the presented hypothesis must be only verified by extra radiocarbon dates and excavations.

A function was of the objects surrounded by ramparts and moats remains an open case. Geoarchaeological data presented above do not supply explain this item. According to Grążawski (2013) such objects could be related to traditional Neolithic circular enclosures, which could also reach the Baltic borderland.

Acknowledgments

The authors would like to thank Professor Leszek Marks and the reviewers for their valuable comments and suggestions. Research on the Radomno Island was made possible thanks to the research project funded by the Polish National Science Centre (NCN): *Correlation of prehistoric and early medieval settlement phases in northeast Poland with the changes of the natural environment in the light of lacustrine sediments study* (ID: UMO-2016/21/B/ST10/03059/ID:335021/no.2016/21/BST10/03059).

REFERENCES

Ackermann, F., 1999. Airborne laser scanning: present status and future expectations. ISPRS. Journal of Photogrammetry and Remote Sensing 54 (2–3), 64–67.

Affek, A., 2016. Past Carpathian landscape recorded in the microtopography. Geographia Polonica 89/3, 415–424.

Aspinall, A., Gaffney, C.F., Schmidt, A., 2008. Magnetometry for Archaeologists. Plymouth Altamira Press, Lanham. New York-Toronto.

Banaszek, Ł., 2014. Airborne laser scanning within Polish archaeology. Is the method's potential being fully exploited. Folia Praehistorica Posnaniensia 19, 207–257.

Challis, K., 2006. Airborne laser altimetry in alleviated landscapes. Archaeological Prospection 13 (2), 103–127.

Conyers, B.L., 2013. Ground-Penetrating Radar for Archaeology. 3rd Edition. Altamira Press.

Conyers, B.L., 2016. Ground-Penetrating Radar for Geoarchaeology. Wiley and Blackwell.

Conyers, B.L., 2016a. Ground-Penetrating Radar Mapping Using Multiple Processing and Interpretation Methods. Remote Sensing 8, 562, doi:10.3390/rs8070562

Conyers, B.L., 2018. Ground-Penetrating Radar and magnetometry for Buried Landscape Analysis. Springer Briefs in Geography. Springer.

Conyers, B.L., Leckebusch, J., 2010. Geophysical archaeology research agendas for the future: Some Ground-penetrating Radar examples. Archaeological Prospection 17, 117–123.

Crow, P., Benham, S, Devereux, B.J, Amable, G.S., 2008. Woodland vegetation and its implications for archaeological survey using LiDAR. Forestry 80, 241–243.

Crutchley, S., Crow, P., 2009. The Light Fantastic: Using airborne laser scanning in archaeological survey, Swindon.

Devereux, B., Amable, G., Crow, P., Cliff, A., 2005. The potential of airborne LiDAR for detection of archaeological features under woodland canopies. Antiquity 79, 648–660.

Doneus, M., Briese, C., 2011. Airborne Laser Scanning in forested areas – potential and limitations of an archaeological prospection technique. Remote Sensing for Archaeological Heritage Management. EAC Occasional Paper 5, 59–76.

Doneus, M., Briese, C., Fera, M., Janner, M., 2008. Archaeological prospection of forested areas using full-waveform airborne laser scanning. Journal of Archaeological Science 35, 882–893.

Ducic, V., Hollaus., M, Ullrich, A., Wagner, W., Melzer, Th., 2006. 3D vegetation mapping and classification using full-waveform laser scanning. In: Koukal, T., Schneider, W. (Eds) In 3-D Remote Sensing in Forestry, 211–218. Vienna.

Evans, J., Hudak, A., Faux, R., Smith, A., 2009. Discrete return LiDAR in natural resources: recommendations for project planning, data processing and deliverables. Remote Sensing 1 (4), 779–786.

Fassbinder, W.E., 2015. Seeing beneath the farmland, steppe and desert soil: magnetic prospecting and soil magnetism. Journal of Archaeological Science 56, 85–95.

Gałązka, D., Skrobot, W., Szarzyńska, A., 2015. Dylewskie Hills, Geology, Anthropology of the space. Mantis, Olsztyn (in Polish).

Gałązka, D., 2009. Explanations to the detailed Geological Map of Poland (1:50 000), Iława sheet 210. Warsaw (in Polish).

Gaffney, C., 2008. Detecting trends in the prediction of the buried past: a review of geophysical techniques in archaeology. Archaeometry 50 (2), 313–336.

Gręźawski, K., 2013. A report from archaeological verification examinations carried out in Radomno in 2011. In: Fudzińska, E. (Ed.) XVIII Sesja Pomorzoznawcza, vol. 1. Od Epoki kamienia do wczesnego średniowiecza. Materiały z konferencji 16–19 listopada 2011, Malbork, 125–131 (in Polish).

Hesse, R., 2010. LiDAR-derived Local Relief Models – a new tool for archaeological prospection. Archaeological Prospection 17 (2), 67–72.

Holliday, V. T., Gartner, W. G., 2007. Methods of soil P analysis in archaeology. Journal of Archaeological Science 34, 301–333.

Karczewski, J., 2007. Introduction to ground-penetrating radar method. AGH, Krakow (in Polish).

Kobyliński, Z. (Ed.), 2017. Catalogue of the Warmia and Masuria settlements. Warszawa (in Polish).

Kurczyński, Z., 2015. Air laser scanning – theoretical basis. In IT System of the Country's Protection Against Extreme Hazards. In: Wężyk, R. (Ed.), A handbook for training participants on the use of LiDAR products. Warsaw, 59–61 (in Polish).

Lasaponara, R., Coluzzi, R., Masini, N., 2011. Flights into the past: full-waveform airborne laser scanning data for archaeological investigation. Journal of Archaeological Science 38, 2061–2070.

Lewis, H., 1999. Micromorphological study of ridge-and-furrow remains at Watson's Lane, Little Thetford, Cambridgeshire (unpublished dissertation), 1–13.

McOmish, D., 2011. Introductions to Heritage Assets: Field Systems. English Heritage 1–5, 1–8.

Owsin, J.A., 2009. Field guide to geophysics in archaeology. Springer.

Report., 2013. Report on the state of forests in Poland Directorate General of State Forests, Poland, Warsaw, 7 (in Polish).

Scollar, I., Tabbagh, A., Hesse, A., Herzog, I., 1990. Archaeological Prospecting and Remote Sensing. Topics in Remote Sensing 2. Cambridge University Press: Cambridge.

Wehr, A., Lohr, U., 1999. Airborne laser scanning – an introduction and overview. ISPRS Journal of Photogrammetry and Remote Sensing 54 (2–3), 68–82.

Welc, F., Lipovac Vrkljan, G., Konestra, K., Rosić, T., 2017a. Remote sensing of a Roman pottery workshop. Report on a geophysical survey carried out in Crikvenica (ancient Ad Turres, Croatia). Studia Quaternaria 34 (2), 119–130.

Welc, F., Mieszkowski, R., Conyers, L.B., Budziszewski, J., Jedynak, A., 2016. Reading of Ground-Penetrating Radar (GPR) images of Prehistoric flint mine: case study from Krzemionki Opatowskie archaeological site in Central Poland. Studia Quaternaria 33 (2), 69–78.

Welc, F., Mieszkowski, R., Lipovac Vrkljan, G., Konestra, A., 2017. An attempt to integration of different geophysical methods (magnetic, GPR and ERT): A Case study from the Late Roman settlement on the Island of Rab (Croatia). Studia Quaternaria 34 (2), 47–59.

Won, I.J., Huang, H., 2004. Magnetometers and electromagnetometers. The Leading Edge 23, 448–451.